Laser Ginzburg-Landau equation and laser hydrodynamics

K. Staliunas*
Physikalisch-Technische Bundesanstalt Braunschweig, Laboratory 4.42, Bundesallee 100, 3300 Braunschweig, Germany
(Received 30 December 1991; revised manuscript received 10 July 1992)

A laser Ginzburg-Landau equation with fourth- and higher-order diffusion terms is derived from the Maxwell-Bloch equations describing a laser. It is shown that the higher-order diffusion terms in the laser Ginzburg-Landau equation are crucial for the transverse structure formation. Laser-hydrodynamical equations are derived, and the correspondence between laser light dynamics and the dynamics of a compressible, viscous, quantized fluid is demonstrated.

PACS number(s): 42.60.Jf, 42.65.−k

I. INTRODUCTION

Recent investigations of multi-transverse-mode lasers have shown similarities between laser dynamics and the dynamics of fluids. In particular, the optical vortices found in laser radiation [1–3] are one of the phenomena with a direct analog in superfluids [4,5]. This analogy hints of the existence of further-reaching correspondences between optics and hydrodynamics.

The similarity finds its explanation in the possibility of reducing the laser equations in a limiting case to the complex Ginzburg-Landau equation (CGLE), and further to hydrodynamic equations. Several attempts have been made in the past to obtain a CGLE describing correctly the dynamics of laser radiation. In [6], the problem was solved for class-A lasers emitting a single longitudinal and transverse mode. The material variables were considered to be enslaved by the electromagnetic field in a "good cavity," and adiabatically eliminated.

In [1,7,8], a CGLE for the multi-transverse-mode laser field (with the dependence on transverse coordinates included) was derived. It possesses diffraction and diffusion terms that communicate information within the laser beam cross section, and give rise to the transverse structure formation.

The CGLE obtained in [1,8] (which at present is regarded as the most precise laser CGLE) possesses a diffusion term that is proportional to the cavity detuning. For negative detuning, the diffusion changes to unphysical "antidiffusion," causing the appearance of field singularities and leading to "blowup" of the solutions. The case of negative detuning is significant because the excitation of higher transverse modes, and with it the generation of nontrivial patterns is achieved experimentally usually for negative detuning [3].

In the present paper, the laser CGLE (LGLE) is derived in a higher-order approximation. It possesses fourth- and higher-order diffusion terms, which prevent the "blowup" for negative detuning. It is shown (Sec. III) that this modified CGLE describes correctly the excitation of transverse modes and structure formation in a laser.

The structure of the LGLE derived in the paper is similar to the structure of the Swift-Hohenberg equation [9], describing in particular the dynamics of convective fluids [10]. Thus the pattern formation in the lasers has the same origin as the convective pattern formation in a fluid layer heated from below, in particular.

In Sec. IV, a further reduction of the LGLE is made to obtain laser hydrodynamical equations. For all laser variables and parameters, the hydrodynamical correspondences are found, which helps to understand the analogy between laser optics and hydrodynamics of a compressible, viscous, and quantized fluid. A vortex flow obtained numerically from the LGLE (Sec. V) illustrates the correspondence.

II. THE LASER COMPLEX-GINZBURG-LANDAU EQUATION

The Maxwell-Bloch equations provide a semiclassical description of the slowly varying fields in a single-longitudinal-mode, ring cavity laser [7]:

$$\frac{\partial E}{\partial t} = -(i\omega_C + \kappa)E + \kappa P + i\alpha\kappa\nabla^2 E \ , \tag{1a}$$

$$\frac{\partial P}{\partial t} = -(i\omega_A + \gamma_\perp)P + \gamma_\perp E D \ , \tag{1b}$$

$$\frac{\partial D}{\partial t} = -\gamma_\parallel[(D - D_0) + \tfrac{1}{2}(E^*P + P^*E)] \ . \tag{1c}$$

Here $E(\mathbf{r},t)$, $P(\mathbf{r},t)$, and $D(\mathbf{r},t)$ are two-dimensional envelopes of electric field, polarization, and population inversion, correspondingly; κ, $\gamma_\perp$, and $\gamma_\parallel$ are decay rates of these variables, $D_0(\mathbf{r})$ is the unsaturated value of population inversion, and the frequencies ω_A and ω_C are the central frequencies of atomic gain line and resonator mode. The vector $\mathbf{r}$ is the position in the plane (r,ϕ) normal to the laser beam propagation direction $\mathbf{z}$.

The term $i\alpha\kappa\nabla^2 E$ in Eq. (1a) is the diffraction term, $\alpha=(4FT)^{-1}$ is the diffraction constant, where $F=\pi r_0^2/(\lambda L)$ is the resonator Fresnel number, r_0 is the resonator mirror radius, L is the full resonator length, λ is the wavelength of the emitted radiation, and T is the resonator mirror transmittivity. The transversal coordinates x and y are normalized to resonator mirror radius r_M.

In the "good-cavity" limit, i.e., when both the polariza-

tion and population inversion are decaying much more quickly than the electromagnetic field ($\kappa \ll \gamma_\perp, \gamma_\parallel$), the former variables can be adiabatically eliminated, and the Maxwell-Bloch equation system (1) can be reduced to a complex Ginzburg-Landau equation (CGLE) [7]:

$$\frac{\partial A}{\partial \tau} = (D_0 - D_{\rm th})(1+i\beta)A + id\nabla^2 A - (1+i\beta)|A|^2 A \ , \tag{2}$$

where $A(\mathbf{r},t)$ is the order parameter proportional to the electromagnetic field: $A(\mathbf{r},t) = E(\mathbf{r},t)(D_0/D_{\rm th})^{1/2}$, where $D_{\rm th} = 1+\beta^2$ is the threshold pump value, and the parameter $\beta = \omega'_C/\kappa$ is the laser resonator detuning, where the frequencies ω'_A and ω'_C are now with respect to a reference frequency $\omega_r = (\kappa\omega_A + \gamma_\perp\omega_C)/(\kappa+\gamma_\perp)$, given by the standard mode pulling formula. The normalized time τ is $\tau = t\kappa/D_{\rm th}$, and the diffraction parameter is $d = \alpha D_{\rm th}$. Equation (2) is valid near the laser threshold: the derivation of the nonlinear term uses a cubic approximation, thus requiring this "near-threshold" assumption.

The solution of the CGLE (2) displays an instability because of the absence of a diffusion term; in particular, in the limit of the large negative β, it becomes the nonlinear Schrödinger equation, which is known in two dimensions to give finite-time blowing up. Thus Eq. (2) is structurally unstable, and even a small diffusion would stabilize it. The diffusive term appears when the polarization is not fully enslaved by the electromagnetic field (e.g., if it is changing with a delay with respect to the field changes). It means that the spectral profile of the amplification line must be considered no more flat than in the adiabatic limit used to derive (2) ($\kappa \ll \gamma_\perp$), but it retains its shape. Thus, in this case, the next approximation for the polarization $P^{(1)}(\mathbf{r},t)$ is calculated from (1b):

$$P^{(1)} = P^{(0)} - \frac{\partial P^{(0)}}{\partial t}(i\omega_A + \gamma_\perp)^{-1} \ , \tag{3}$$

where $P^{(0)}(\mathbf{r},t)$ is the zero-order approximation for the polarization used to eliminate it adiabatically when deriving (2):

$$P^{(0)} = (1+i\beta)\frac{ED}{D_{\rm th}} = (1+i\beta)\frac{ED_0}{D_{\rm th}+|E|^2} = (1+i\beta)\frac{ED_0}{D_{\rm th}}(1-|E|^2/D_{\rm th}) \ . \tag{4}$$

Note that the cubic approximation is used in the last expression in (4).

The polarization time derivative $\partial P^{(0)}/\partial t$ is calculated from (4) and (1a) to obtain the corrected value of polarization $P^{(1)}$. The correcting terms appear to be of the higher order of smallness in the "good-cavity" approximation ($\kappa \ll \gamma_\perp$). Only the correcting term including ∇^2 in a linear way is relevant:

$$P^{(1)} = P^{(0)} - id\eta(1+i\beta)^2\frac{D_0}{D_{\rm th}^2}\nabla^2 E \ ; \tag{5}$$

here $\eta = \kappa/\gamma_\perp$ is the cavity finesse parameter. Note that the nonlinear term containing $\nabla^2(E|E|^2)$ is dropped in (5) because of its smallness compared with the term that contains $\nabla^2 E$ in a linear way. The expression (5) is then again inserted into (1a) to obtain

$$\frac{\partial A}{\partial \tau} = (D_0 - D_{\rm th})(1+i\beta)A + (id+d_2)\nabla^2 A - (1+i\beta)|A|^2 A \ , \tag{6}$$

where all terms are defined as in (2), and the diffusion coefficient is $d_2 = \alpha 2\beta\eta D_0/D_{\rm th}$.

Equation (6) is the CGLE in its classical form, and also was derived before [1,8] from the laser equations using the central manifold technique. Equation (6) was used to investigate dynamics of optical vortices in a laser in the case of positive detuning β. But, as noted before, negative detuning $\beta < 0$ produces unphysical "antidiffusion," causing the "blowup" of the solutions.

This "blowup" can be prevented using the next higher corrections for the polarization:

$$P^{(n)} = P^{(n-1)} - \frac{\partial P^{(n-1)}}{\partial t}(i\omega_A + \gamma_\perp)^{-1} \ , \tag{7}$$

and after the same procedure as was used to obtain (5) and (6), the polarizations of higher order are calculated:

$$P^{(n)} = P^{(0)} + (1+i\beta)\frac{D_0}{D_{\rm th}}\sum_{n=1}^{\infty}\left[-\frac{id\eta}{D_{\rm th}^2}(1+i\beta)\nabla^2\right]^n E \ , \tag{8}$$

and the following equation of the CGLE family is derived:

$$\frac{\partial A}{\partial \tau} = (D_0 - D_{\rm th})(1+i\beta)A + id\nabla^2 A - (1+i\beta)|A|^2 A + D_0\left[(1+i\beta)\sum_{n=1}^{\infty}\left[-\frac{id\eta}{D_{\rm th}^2}(1+i\beta)\nabla^2\right]^n\right]A \ . \tag{9}$$

Noting that the diffusion term series is formally a geometric progression, Eq. (9) can be rewritten in a more compact form:

$$\frac{\partial A}{\partial \tau} = (D_0 - D_{\rm th})(1+i\beta)A + id\nabla^2 A - (1+i\beta)|A|^2 A - D_0\left[\frac{(1+i\beta)\sigma\nabla^2}{1+\sigma\nabla^2}\right]A \ ; \tag{10}$$

here σ is defined as $\sigma = id\eta(1+i\beta)/D_{\rm th}^2$. Due to the presence of the higher-order diffusion terms, Eq. (10) is no longer a CGLE in its classic form, and will be referred to as the laser Ginzburg-Landau equation (LGLE).

Equation (10) is derived in the good-cavity limit $\eta \ll 1$. On the other hand, η is nonzero, since the finite width of the amplification line is taken into account in (10). Thus (10) is valid for class-A lasers with an amplification line broader than the resonator mode, and than the transverse-mode separation.

In order to simplify (9) and (10), the infinite series of higher-order diffusions can be truncated. As shown in Sec. III, the truncation to the fourth-order diffusion term retains all the basic properties of the LGLE:

$$\frac{\partial A}{\partial \tau} = (D_0 - D_{\rm th})(1+i\beta)A + (id + d_2)\nabla^2 A + d_4 \nabla^4 A - (1+i\beta)|A|^2 A \ , \tag{11}$$

where $d_4 = -\alpha^2 \eta^2 D_0 / D_{\rm th}$ is a fourth-order diffusion coefficient, and Eq. (11) will be referred to as CGLE IV throughout the paper.

Note that the second- and fourth-order diffusion terms in (11) can be rewritten in the form $d_4(\gamma + \nabla^2)^2 - d_4\gamma^2$, where $\gamma = d_2/(2d_4)$. This is exactly as the diffusion term in the Swift-Hohenberg equation [9] used to describe convective fluid dynamics. (The formation of Reyleigh-Bénard convective patterns in a fluid layer heated from below are described by these equations correspondingly [10].) The pattern-formation processes in CGLE IV, therefore, can be expected to be similar to those in convective fluids.

Before the properties of the solutions of Eqs. (10) and (11) are investigated, some terms must be added phenomenologically to obtain better correspondence with a real laser. Characteristic for the real lasers is a pump nonuniformly distributed in space (often of Gaussian spatial profile), and the presence of curved (spherical) mirrors. With the pump profile $\mu_1(\mathbf{r}) = \exp(-r^2/r^2_{\rm pump})$ [corresponding to the unsaturated population inversion of the form $D_0(\mathbf{r}) = D_0 \mu_1(\mathbf{r})$], and the curved mirrors causing the phase shift (phase gain) $\partial\Phi/\partial\tau = \mu_2(\mathbf{r})$, one finally obtains for CGLE IV:

$$\frac{\partial A}{\partial \tau} = [(D_0\mu_1(r) - D_{\rm th})(1+i\beta) + i\mu_2(r)]A + (id + d_2)\nabla^2 A + d_4\nabla^4 A - \mu_1(r)(1+i\beta)|A|^2 A \ , \tag{12}$$

and correspondingly for the LGLE:

$$\frac{\partial A}{\partial \tau} = [(D_0\mu_1(r) - D_{\rm th})(1+i\beta) + i\mu_2(r)]A + id\nabla^2 A - D_0\mu_1(r)\left[\frac{(1+i\beta)\sigma\nabla^2}{1+\sigma\nabla^2}\right]A - \mu_1(r)(1+i\beta)|A|^2 A \ . \tag{13}$$

The phase gain profile caused by the curved mirrors is of the form $\mu_2(r) = -ar^2$, where $a = Ff^2 D_{\rm th}/T$. Parameter f is the cavity mirror curvature parameter depending on the cavity configuration: for stable cavities it varies from 0 (plane mirror cavity) to 2 (concentric mirror cavity); for a confocal cavity, e.g., $f = 1$.

To check the validity of definitions of parameters a and d, Eqs. (12) and (13) were linearized, and the parameters of fundamental Gaussian mode $\rm TEM_{00}$ were calculated to yield the beam radius $r_b^2 = 2(d/a)^{1/2} = (Ff)^{-1}$ (the distance is normalized to the radius of the mirror), and the frequency $\omega_0 = -2(ad)^{1/2} = -fD_{\rm th}/T$ (the frequency is normalized to the width of the cavity mode divided by $D_{\rm th}$; it is also the separation of transverse modes). The product $r_b^2\omega_0 = -4d$ does not depend on the focusing parameter f, as it ought to be in lasers.

Note that the definition of parameters a and d is different from the careful derivation in [11], since the distances, for convenience, are normalized to the mirror radius r_M here. Nevertheless the definitions here are compatible with those in [11].

III. LGLE INSTABILITIES

One of the simplest ways to obtain information about the capability of a nonlinear system to generate spatial structures is the linear stability analysis of its homogeneous solutions. Such an analysis was performed for the LGLE (10) and the CGLE IV (11) with spatially homogeneous parameters. The equations were linearized around the trivial solution $A(\mathbf{r}) = 0$, and the growth exponents for the spatial modes were calculated:

$$\lambda_{\rm CGLE\ IV} = D_0 - D_{\rm th} - D_0(2\beta k'^2 + D_{\rm th} k'^4) \ , \tag{14a}$$

$$\lambda_{\rm LGLE} = D_0 - D_{\rm th} - D_0 k'^2 \frac{2\beta + k'^2 D_{\rm th}}{(1+\beta k'^2)^2 + k'^4} \ ; \tag{14b}$$

here $\lambda_{\rm CGLE\ IV}$ and $\lambda_{\rm LGLE}$ are the real parts of eigenvalues in the linear stability analysis for Eqs. (11) and (10), correspondingly, and k' is a normalized spatial wave number: $k'^2 = k^2 \alpha\eta / D_{\rm th}$.

In the case of positive detuning ($\beta > 0$), the perturbation with $k' = 0$ has the maximal growth exponent, as Eqs. (14a) and (14b) show. This means that if the laser is above generation threshold ($D_0 > D_{\rm th}$), the plane wave with the wave vector parallel to the laser axis will grow fastest and will largely define the stationary pattern in the laser beam cross section. (The stationary pattern in this case $\beta > 0$ is trivial: a homogeneous spatial distribution). In the case of negative β, according to (14), the modes with particular (nonzero) transverse wave number k become unstable and grow. The growth rates depending on the transverse wave number k are given in Fig. 1 for the CGLE IV and the LGLE. The corresponding curve for the classical CGLE (6) is also given. The latter shows that all short-wavelength perturbations are unstable and grow, thus causing "blowup" of the solutions of Eq. (6) for $\beta < 0$.

In Eqs. (10) and (11) for $\beta < 0$, the waves propagating at

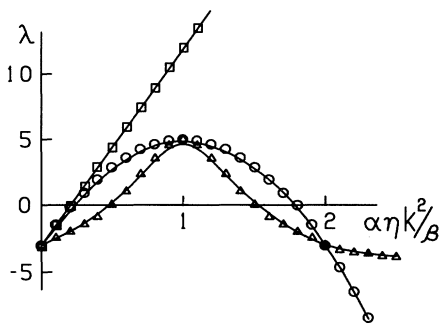

FIG. 1. Stability analysis of the trivial solution $A(\mathbf{r}) = 0$: perturbation growth exponents vs perturbation wave number for the different laser models: □—classical CGLE (6), ○—CGLE IV(11), △—LGLE (10) (coinciding with the corresponding curve for the full MBE system in case of $\gamma_\parallel, \gamma_\perp \gg \kappa$). The parameters are $\beta = -2$, $D_0 = 2$.

a particular nonzero angle to the optical axis of the laser are most strongly amplified, and will prevail in the generated radiation (see also [12], for a case of full MBE system). In the case of a real laser [models (12) and (13) together with corresponding boundary conditions], these "tilted waves" will arrange in standing or traveling waves, and correspondingly a nontrivial stationary or dynamic pattern will occur in the cross section of the laser beam.

The corresponding stability analysis was performed for the initial MBE system (1), too. The dependence of the perturbation growth exponent on transverse wave number k for the full laser equations coincides with good accuracy with the corresponding curve for the LGLE (the difference is less than 3–5%).

The following point is worth noting: due to the nonlinear coupling of the electromagnetic radiation with the material variables, as well as due to radiation diffraction, the spectral amplification profile is transformed into the transversal wave vector (k) domain in the case of negative detuning. As can be seen from expressions (14) and from Fig. 1, the Lorenzian gain line profile reappears in the k space for the LGLE. In the case of the CGLE IV, the Lorenzian growth exponent curve is approximated by a second-order polynomial. It is found that this difference does not alter the qualitative features (see, e.g., the numerical results in Figs. 2 and 3) of the transverse structure formation. The classical CGLE's (2) and (6), in fact, approximate the Lorenzian gain line by lower-order polynomials (the zero- and the first-order, correspondingly). This permits one to understand why these equations are not capable of describing the laser transverse dynamics correctly.

For the most unstable wave number k_0, both expressions in (14) yield

$$k_1^2=\frac{D_{\rm th}}{\alpha\eta}k_0'^2=-\frac{\beta}{\alpha\eta}\ . \tag{15}$$

This coincides with the expression for the case of the full laser equations (see also [12] for the MBE case).

In the case of small negative detuning, only the modes of long wavelength become unstable; this causes no modulation of the laser beam until the maximum-instability wavelength is smaller than the beam radius. With increasing negative detuning, the maximum-instability wavelength decreases. When it becomes comparable with the characteristic spatial modulation length of the next higher transverse laser mode, the instability destroys the initial Gaussian field distribution, and the laser switches to a higher transverse mode (TEM_{01}^*—so called "doughnut" for a cylindrically symmetric laser). Further increase of negative detuning makes the maximum-instability wavelength comparable with the spatial modulation length of the next transverse-mode family, etc. Thus the mode (and transverse structure) formation in a laser beam may be well explained with the help of the LGLE (12),(13).

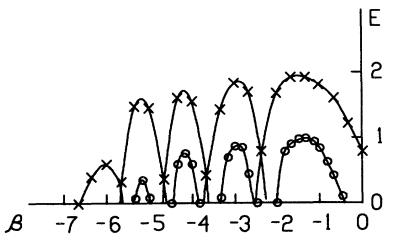

FIG. 2. Laser intensity vs resonator detuning for two different pump values: ○—$D_0=2.6$, ×—$D_0=3.0$. CGLE IV (11) with the following parameters was calculated: $\eta=0.2$, $T=0.05$, $f^2=0.5$, $F=10$. The pump profile $\mu_1(\mathbf{r})$ was of Gaussian form with $r_{\rm pump}=0.5$ (normalized to mirror radius).

The numerically calculated total power of radiation emitted by the laser (integration of the CGLE IV), is given in Fig. 2, as a function of detuning β. The excitation of a few transverse-mode families is evident, indicating that the CGLE IV can describe the transverse dynamics of the laser.

In addition to the structure formation discussed, which results from the short-wavelength instability of the zero solution, there exists another structure-forming instability in the laser. It is an instability of the homogeneous nonzero solution (Benjamin-Feir or modulation instability; in the case of model (1), this instability has been first pointed out and analyzed in [7]). From the sideband perturbation analysis of the homogeneous solution $A(\mathbf{r})=(D_0-D_{\rm th})^{1/2}$ for the pure CGLE (2), one obtains

$$\lambda=D_{\rm th}-D_0\pm[(D_0-D_{\rm th})^2-2\beta\alpha D_{\rm th}(D_0-D_{\rm th})k^2 -\alpha^2D_{\rm th}^2k^4]\ . \tag{16}$$

This yields the wave number of maximum instability:

$$k_2^2=-\beta\frac{D_0-D_{\rm th}}{\alpha D_{\rm th}}\ . \tag{17}$$

For the sake of simplicity, the sideband perturbation analysis was performed here for the pure CGLE (2). The more effortful analysis for the modified CGLE (6), (10), and (11) was performed numerically and yielded approximately the same result.

This latter structure formation occurs as a result of a combination of the imaginary part of the nonlinear term and the diffraction term in Eqs. (2), (6), (10), and (11). The instability due to this mechanism is self-focusing. (Self-focusing of light is a result of a combination of a Kerr-type nonlinearity and diffractive propagation: it causes the well-known intensity singularities in two-dimensional cases [13], and optical soliton formation in one-dimensional cases [14].) In the classical CGLE theory, this mechanism leads to the spatial instability [15] and is considered as a principal mechanism leading to the structure formation and turbulence of the CGLE. It turns out, though, that at least in class-A lasers, where $\eta\ll1$, near the laser threshold, structure formation is mainly caused by the first mechanism—the short-wavelength instability. The ratio of wave numbers of maximal instabilities relating to both mechanisms is

$$k_2^2/k_1^2=\eta\frac{D_0-D_{\rm th}}{D_{\rm th}}\ . \tag{18}$$

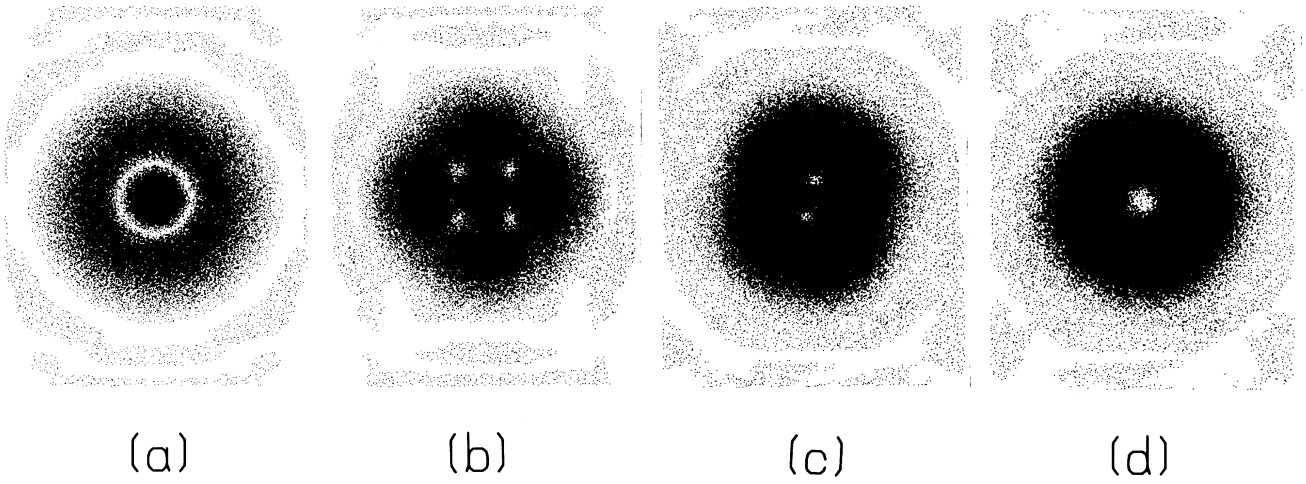

FIG. 3. Metastable patterns (a), (b), (c), and the stable pattern (d) appearing during numerical integration of the CGLE IV. The initial field distribution was homogeneous; the parameters used are as for Fig. 2 and $\beta=-4.25$, $D_0=3.0$. States (a)–(d) are the steady states of the laser as calculated by mode expansion and experimentally observed in [3].

This means that, in the case $D_0\eta \gg D_{\text{th}}$, the instability caused by self-focusing (Benjamin-Feir instability) dominates the structure formation in the laser, the short-wavelength instability caused by the limited width of the laser gain line (the laser instability) being less important. Usual operating conditions for a class-A laser are $D_0\eta \ll D_{\text{th}}$, thus the pattern formation in such lasers has a different origin from the one in the classical CGLE.

To end this section, additional evidence of the capability of the modified CGLE to describe the transverse pattern formation in lasers is given. Figure 3 shows numerically obtained distributions of laser field intensity. These are the steady-state patterns emitted by a laser tuned to the transverse-mode family $2p+l=2$. These are as found in experiments and mode expansion calculations for different pump strengths and diameters [3]. (Here p is the radial and l the angular index of the Gauss-Laquerre modes.) When the state d is stable, the transverse distribution of the laser radiation is found to evolve through the patterns (a), (b), (c), to the final state (d), after the laser is switched on, as shown in Fig. 4 for the particular laser parameter set. It appears that the patterns (a), (b), (c), which under these conditions are unstable, actually behave metastably. If the laser parameters are changed (width of spatial pump profile, pump intensity), the laser emission evolves towards another one of the patterns shown as the final state.

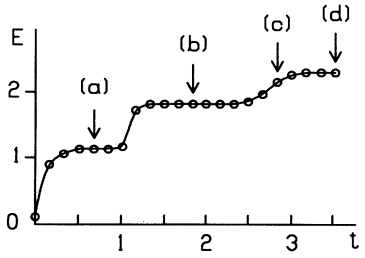

FIG. 4. Intensity of the CGLE IV solution evolving in time. The parameters are as in Fig. 3. The plateaus correspond to the existence of indicated metastable patterns.

It must be noted that the results in Figs. 3 and 4 were obtained, not in the mode expansion calculations as in [3], but by solving numerically partial differential equations.

IV. LASER HYDRODYNAMICAL EQUATIONS

Some features of transverse laser pattern dynamics resemble the dynamics of fluids. In particular, the existence of optical vortices found in lasers [1–3] has a direct counterpart in superfluids [4,5]. This analogy hints of the existence of further-reaching correspondence between optics and hydrodynamics. A formal mathematical analogy is difficult to show with the full laser equation system (1). The LGLE and CGLE IV derived in the previous sections, however, are structurally more similar to hydrodynamic equations, and can consequently be used as a connection between laser optics and hydrodynamics.

As mentioned, the diffusion terms in CGLE IV are analogous to those in the Swift-Hohenberg [9] equation. Consequently, the structure formation in lasers must be similar to the one in convective hydrodynamics describable by the model.

The CGLE in the form (2) is used to describe the dynamics of the order parameter in superfluids [4,5], where the intensity $|A|^2$ corresponds to the fluid density, and the gradient of the field phase $\nabla\Phi$ to the fluid velocity $\mathbf{u}$. The LGLE also can be rewritten in terms of these fluid

parameters, and the dynamical equations for "laser photonic gas" dynamics can be obtained.

The correspondence between the laser equations (1) and compressible superfluid equations of motion has recently been investigated in a limiting case in [16]. Here the purpose is to obtain "laser-fluid" dynamics equations for more general cases.

Rewriting Eq. (12) in terms of $\rho=|A|^2$ and $\Phi=\arg(A)$, analogically as in [16], and separating the real and imaginary parts, one obtains

$$\frac{\partial\rho}{\partial t}=2(D_0\mu_1-D_{\rm th})\rho-2d\nabla\cdot(\rho\nabla\Phi)-2\mu_1\rho^2\ , \tag{19a}$$

$$\frac{\partial\Phi}{\partial t}=\mu_2+\beta(D_0\mu_1-D_{\rm th})+d_4\nabla^4\Phi+d_2\left[\nabla^2\Phi+\nabla\Phi\cdot\frac{\nabla\rho}{\rho}\right]+d\left[\frac{\nabla^2\rho}{2\rho}-\frac{(\nabla\rho)^2}{4\rho^2}-(\nabla\Phi)^2\right]-\beta\mu_1\rho\ ; \tag{19b}$$

here all terms with factors d_2,d_4 in (19a) and with factor d_4 in (19b) have been omitted because of their smallness ($d_4\ll d_2\ll d$), except for the significant one: $d_4\nabla^4\Phi$, in (19b).

Equations (19) are of the form of hydrodynamical equations. The first one is a continuity equation (with spatially distributed sources and sinks corresponding to the amplification and saturation in the laser media); the second one is the Euler equation analog. A further simplification of system (19) is possible in a case of zero detuning ($\beta=0$):

$$\frac{\partial\rho}{\partial t}=2(D_0\mu_1-D_{\rm th})\rho-2\mu_1\rho^2-\nabla\cdot(\rho\nabla\Phi)\ , \tag{20a}$$

$$\frac{\partial\mathbf{u}}{\partial t}+\nabla\frac{(\mathbf{u})^2}{2}=-\nu_4\nabla^4\mathbf{u}-\nabla V(\mathbf{r})-\nabla p/\rho\ . \tag{20b}$$

The transverse coordinate r has been renormalized here: $r^2/2d\rightarrow r^2$, and the velocity $\mathbf{u}$ is $\mathbf{u}=\nabla\Phi$. The parameter $\nu_4=\eta^2D_0/(4D_{\rm th}^3)$ is the fourth-order viscosity parameter (the second-order viscosity is zero for zero detuning). The function $V(\mathbf{r})=-\mu_2(\mathbf{r})=ar^2$ is the effective external force potential due to the inhomogeneous phase gain [curved mirrors in the laser, as introduced in Eqs. (11) and (12), Sec. II]. The internal pressure $p(\mathbf{r},t)$ is a function of the "laser photonic gas" density $\rho(\mathbf{r},t)$ and density gradient $\nabla\ln[\rho(\mathbf{r},t)]$, and is defined by the following differential expression:

$$\delta p=-\rho\delta\left[\frac{\nabla^2\ln(\rho)}{4}+\frac{[\nabla\ln(\rho)]^2}{8}\right]\ . \tag{21}$$

Equations (20) describe the dynamics of a "laser photonic gas" enclosed in the potential well $V(\mathbf{r})$, in the presence of spatially distributed sources and sinks. The gas is compressible and viscous as seen from (20) and (21). In the case of negative detuning, the additional convective forces are present, where the detuning is the direct analog to the temperature gradient in corresponding hydrodynamical systems.

The parameter that defines the complexity of a hydrodynamical system is the Reynolds number $\mathrm{Re}=Lv/\nu$ [4,17]. Here L, v, and ν are characteristic length, velocity, and viscosity in the system. For the characteristic viscosity, $\nu=\nu_4^{1/2}=\eta D_0^{1/2}$ is used (the square root is needed to retain the nondimensionality of Re); the characteristic spatial dimension of the system is the laser beam diameter $2r_B$, and characteristic velocity is evaluated from (20a) in a stationary case ($\partial\rho/\partial t=0$): it is the maximal radial velocity of "laser photonic gas" flow in the case of a flat pump: $v=r_B(D_0-1)$. Then

$$\mathrm{Re}=\frac{D_0-1}{D_0^{1/2}}\frac{r_B^2}{\alpha\eta}\ . \tag{22}$$

The threshold for the Nth transverse-mode family is $D_N=1+[\omega_0\eta(N+1)]^2$ (for zero detuning!), and the beam radius is roughly $r_B=r_0(N+1)^{1/2}$, where ω_0 is the mode frequency separation, and r_0 is the radius of TEM_{00} mode as found in Sec. II. Then taking into account the relation between r_0 and ω_0: $r_0^2\omega_0=-4d$, the laser Reynolds number is $\mathrm{Re}=4(N+1)^2$, if the laser is above threshold for the Nth transverse mode.

It is suggested that the expression of the laser Reynolds number can be formally extended into the region of $\beta<0$, where the short-wavelength instability of the "laser photonic gas" occurs. The laser Reynolds number is then proportional to the square of the number of the transverse-mode families above the threshold under the particular operating conditions [in Fig. 5, the laser Reynolds numbers in the plane (β,D_0) are given].

The maximum Reynolds number for a particular laser configuration is proportional to the square of the highest transversal-mode family possible to excite, and is given by the Fresnel number: $\mathrm{Re}_{\max}=4F^2$.

An explicit analytic expression of the density profile, allowing a solution for $\beta\simeq0$ from (19), does not exist in general. (It can be found in a perturbative way as in [18].) Numerical solutions show that the density (as well

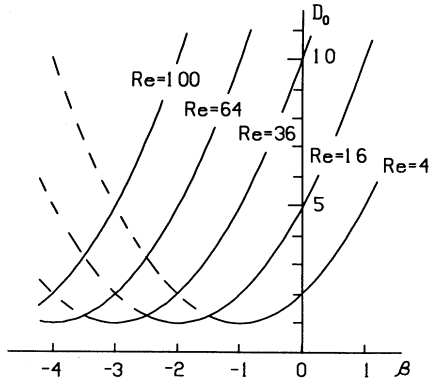

FIG. 5. Laser Reynolds number as a function of pump D_0 and detuning β. The cavity focusing parameter $f^2=0.4$ (chosen to make the transverse-mode frequency separation $\Delta\beta=1$).

as the pressure) is maximal in the middle of the potential well, and decreases with the radial coordinate r, while the distribution of both variables is roughly Gaussian. Such a stationary distribution of laser fluid density corresponds to the Gaussian beam of the fundamental TEM_{00}-mode shape.

Another stationary solution of the system (19),(20) is the vortex solution, which in the limit $r \to 0$ is of the following asymptotic form:

$$\rho(\mathbf{r}) = \frac{r^2}{r_{\text{core}}^2}, \quad \mathbf{u} = \frac{(\mathbf{m} \times \mathbf{r})}{r^2} ; \tag{23}$$

here $\mathbf{m}$ is a unit vector transverse to the plane (r, ϕ) and directed upwards (along the $\mathbf{z}$ axis) for a vortex with positive charge, and downwards for a negative charge; r_{core} is the characteristic vortex radius. Such vortices (with a vanishing density and a infinite fluid velocity at the center) were found in lasers recently [1–3].

Detailed investigations of optical vortex behavior, described by the LGLE equations (10)–(13) and the laser hydrodynamics equations (19),(20), will be given elsewhere (see also [18,19]). It is noted here that the forces causing the optical vortex drift have direct counterparts in hydrodynamics. For example, the radial motion of a single vortex in a laser beam cross section is easily interpreted as a drift caused by radial "laser photon gas" flow. (There is, in general, a nonzero radial flow in a stationary distribution because of the presence of sources and sinks.) On the other hand, the angular circling of a vortex around the optical axis of the laser beam (observed experimentally [20] and numerically investigated [18–20]) can be interpreted as a Magnus drift caused by a buoyancy force. (The vortex is a hollow object and thus experiences a buoyancy caused by the internal pressure gradient and directed away from the laser beam center. The Magnus drift of the rotating object is directed perpendicularly to the force acting on the object and causes a circling of the vortex around the optical axis of the laser in this case.)

The optical vortex is supported by the topological constraint; thus it is extremely stable (it cannot be destroyed alone—just two vortices of opposite topological charge can annihilate). This allows one to consider the "laser photonic gas" as a quantized one, like the superfluid [4,5]. On the other hand, the laser hydrodynamical equations (20) and optical vortex interaction [18] in the lasers show the presence of viscosity. These two facts suggest that the laser photonic gas is similar to a two-component superfluid, where the superfluid and normal-fluid components are simultaneously present, as in finite-temperature superfluid heliumII [4,5].

It is also noted that the existence of a single vortex circling in the laser beam is connected with the excitation of modes TEM_{00} and TEM_{01}^{*} simultaneously; it thus corresponds to a laser Reynolds number: $\text{Re} \cong 20$. It is well known in hydrodynamics that the existence of vortices requires approximately the same minimal value of the Reynolds number of the system [17].

On the other hand, turbulence in hydrodynamics sets in if the Reynolds number of the system exceeds $\cong 2000$. This means that real turbulence in optics (defect-mediated turbulence [21]?) will occur under conditions in which the $N \cong 20$–30-mode family can be exited (or the average number of the vortices N_V is roughly more than $N_V \cong N^2 \cong 500$).

V. THE KARMAN VORTEX STREET IN LASER RADIATION

In this section, a numerical simulation example is given, to illustrate the correspondence between lasers and fluids. The idea to generate numerically a vortex street behind a moving obstacle in a superfuid was given in [22], where the nonlinear Schrödinger equation was studied. Here the LGLE (13) is investigated. Here the "laser photonic gas" flow is created by introducing an inhomogeneous phase gain function, depending linearly on the trans-

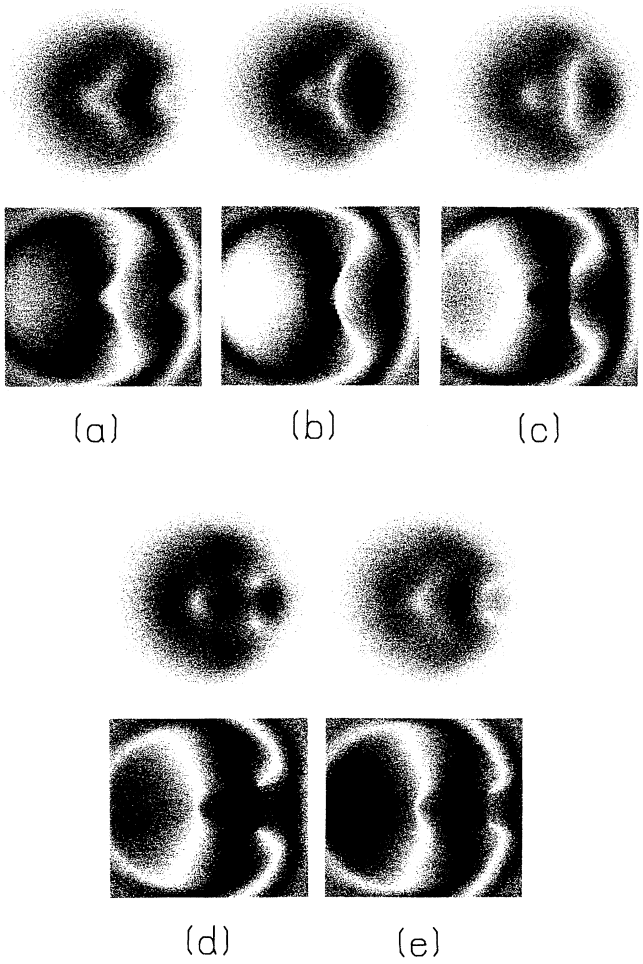

FIG. 6. Intensity and sine-of-phase snapshots of vortex generation behind the obstacle: temporal sequence of a vortex-pair generation period. The parameters of the laser are $F=10$, $f^2=0.1$, $\eta=0.1$, $T=0.1$, $D_0=10$, $\beta=0$, $b=5a$, $r_{\text{pump}}=0.5$, $r_{\text{hole}}=0.05$. The temporal step between snapshots is $\Delta\tau=0.075$. The white spot in the center of the intensity snapshots (upper pictures) corresponds to a hole in one mirror; the "laser photonic gas" flow caused by mirror tilting is directed to the right.

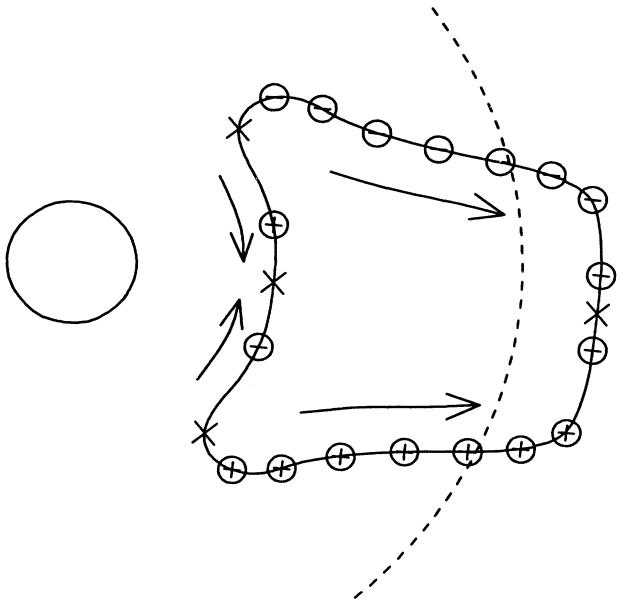

FIG. 7. Trajectories of the vortices generated behind the obstacle in the flow. The crosses mark the positions where the vortex pairs are generated or annihilated. The dotted arc indicates the half-intensity contour line of the laser beam; the solid circle represents the mirror hole. The parameters are as in Fig. 6.

verse coordinate $\mathbf{x}$: $\mu_2'(\mathbf{r})=-ar^2+bx$. In a laser, this can be realized by tilting of a mirror. A circular obstacle was created numerically by introducing higher losses in a circular area around the laser axis (a "hole" in the center of one of the resonator mirrors): $\mu_1'(\mathbf{r})=\exp(-r^2/r_{\text{pump}}^2)-\exp(-r^2/r_{\text{hole}}^2)$.

In Fig. 6, the temporal sequence of radiation intensity and sine-of-phase is presented. The periodic generation of optical vortices (the white spots in the intensity picture and phase singularities in the sine-of-phase picture) is clearly observed. A cavity with Fresnel number $F=10$ was assumed, which does not allow one to observe simultaneously more than two vortex pairs in the laser beam cross section. The Fresnel number (and the corresponding Reynolds number) is too small. This case, however, is close to experiments, where large Fresnel numbers are usually difficult to obtain.

Figure 7 gives the trajectories of the vortices. It is seen that two vortex pairs are generated behind the obstacle in the stream. Two of the vortices are caught by the stream and are carried away from the obstacle, while two other vortices quickly annihilate in the deadwater of the obstacle.

The numerical calculation shows that the vortex generation occurs when the laser flow velocity (phase gradient induced by laser mirror tilting) is beyond a threshold value. The corresponding threshold Reynolds number ($\text{Re}'=r_{\text{hole}}v_{\text{tilt}}/\nu$, where r_{hole} is a radius of the hole in the cavity mirror, and $\mathbf{v}_{\text{tilt}}=\nabla\Phi$ is the numerically evaluated velocity of the laser photonic gas flow due to mirror tilting) is approximately $\text{Re}'_{\text{th}}\cong 40$ and again corresponds well to the minimal Reynolds number in hydrodynamics to generate the Karman vortex street [17].

Further increase of flow velocity leads to quasiperiodic dynamics, and to irregular (chaotic) vortex-pair generation.

ACKNOWLEDGMENTS

The author thanks C. O. Weiss for numerous discussions and help with the manuscript, L. Gil and S. Rica for sharing the unpublished results and suggesting the vortex street idea, and L. A. Lugiato for useful discussions. The author received support from the Alexander von Humboldt Foundation. The work was partially supported by ESPRIT Basic Research Action TONICS.

*Permanent address: Department of Quantum Electronics, Vilnius University, Sauletekio av.9, corp. 3, 2054 Vilnius, Lithuania.

[1] P. Coullet, L. Gil, and F. Rocca, Opt. Commun. **73**, 403 (1989).
[2] F. T. Arecchi, G. Giacomelli, P. L. Ramazza, and S. Residori, Phys. Rev. Lett. **65**, 2531 (1990).
[3] M. Brambilla, F. Battipede, L. A. Lugiato, V. Penna, F. Prati, C. Tamm, and C. O. Weiss, Phys. Rev. A **43**, 5090 (1991).
[4] R. L. Donelly, *Quantized Vortices in Helium II* (Cambridge University Press, Cambridge, England, 1991).
[5] E. B. Sonin, Rev. Mod. Phys. **59**, 87 (1987).
[6] R. Graham and H. Haken, Z. Phys. **237**, 31 (1970).
[7] L. A. Lugiato, C. Oldano, and L. M. Narducci, J. Opt. Soc. Am. B **5**, 879 (1987).
[8] G.-L. Oppo, G. D'Alessandro, and W. Firth, Phys. Rev. A **44**, 4712 (1991).
[9] J. Swift and P. C. Hohenberg, Phys. Rev. A **15**, 319 (1977).
[10] C. Perez-Garcia, *Stability in Thermodynamic Systems* (Springer-Verlag, Berlin, 1983).
[11] L. A. Lugiato, G. L. Oppo, J. R. Tredicce, L. M. Narducci, and M. A. Pernigo, J. Opt. Soc. Am. B **7**, 1019 (1990).
[12] P. K. Jakobsen, J. V. Moloney, A. C. Newell, and R. Indik, Phys. Rev. A **45**, 8129 (1992).
[13] V. E. Zacharov and A. B. Shabat, Zh. Eksp. Teor. Fiz. **61**, 118 (1971) [Sov. Phys. Lett. **34**, 62 (1972)].
[14] A. Hasegava and F. Tappert, Appl. Phys. Lett. **23**, 142 (1973).
[15] Y. Kuramoto, in *Chemical Oscillations, Waves and Turbulence* (Springer, New York, 1984).
[16] M. Brambilla, L. A. Lugiato, V. Penna, F. Prati, C. Tamm, and C. O. Weiss, Phys. Rev. A **43**, 5114 (1991).
[17] L. M. Milne-Thompson, *Theoretical Hydrodynamics* (Macmillan, London, 1955).
[18] K. Staliunas, Opt. Commun. **90**, 123 (1992).

[19] C. O. Weiss, Chr. Tamm, and K. Staliunas, *Dislocations in Laser Fields, in Evolution of Dynamical Structures in Complex Systems* (Springer-Verlag, Berlin, 1992).

[20] M. Brambilla, M. Cattaneo, L. A. Lugiato, R. Pirovano, F. Prati, A. J. Kent, G. L. Oppo, A. B. Coates, C. O. Weiss, C. Green, E. J. D'Angelo, and J. R. Tredicce (unpublished).

[21] P. Coullet, L. Gil, and J. Lega, Phys. Rev. Lett. **62**, 1619 (1989).

[22] Th. Frisch, Y. Pomeau, and S. Rica, Phys. Rev. Lett. **69**, 1644 (1992).